

COMPUTATIONAL FLUID DYNAMICS FOR THE ANALYSIS OF LIGHT WATER REACTOR FLOWS

Constantine P. Tzanos

Argonne National Laboratory
9700 S. Cass Avenue, Building 208
Argonne, Illinois 60439 USA
tzanos@anl.gov

ABSTRACT

Benchmark experiments simulating flows in a PWR rod bundle were analyzed to evaluate the performance of a state of the art computational fluid dynamics (CFD) code. For the simulation of turbulence a number of standard $k-\epsilon$ models were used. Away of components that cause significant flow deflections the difference between mean velocity predictions and measurements is within the experimental error. Close to such components there is significant discrepancy between velocity predictions and measurements. Even in rod bundles without flow deflectors, the turbulence predictions of standard $k-\epsilon$ models are in significant discrepancy with measurements. These discrepancies are greater close to components that cause flow deflections. Turbulence generated by vanes on spacer grids significantly enhances thermal mixing. To improve the fidelity of CFD simulations of flows in reactor rod bundles the development of RANS turbulence models based on such flows is needed.

1.0 INTRODUCTION

The established thermal-hydraulics computer codes currently used in the nuclear industry are mainly 1-D with limited 2-D or 3-D capabilities, and are limited to Cartesian or cylindrical grids. The momentum equations solved by these codes are the Euler (inviscid) equations, instead of the basic Navier-Stokes equations, and wall friction and heat transfer are evaluated from empirical correlations. Similarly, turbulence is handled empirically through the use of friction and heat transfer coefficients. Reactor fuel-bundle geometries are very complex and cannot be represented faithfully by Cartesian or cylindrical grids. Flows and heat transfer in these bundles are three-dimensional, and thermal mixing, which is driven by cross-flows and turbulence, has a very significant impact on economic and safety performance.

Advances in computational fluid dynamics (CFD), turbulence simulation, and parallel computing have made feasible the development and application of three-dimensional (3-D) CFD codes that can simulate fluid flow and heat transfer in realistic reactor geometries with significantly reduced reliance, especially in single phase, on empirical correlations. These codes hold the promise for adequately accurate simulation of flows and heat transfer in reactor fuel bundles, that can significantly reduce the need for expensive experiments for bundle design optimization, and reduce conservatism in safety margins.

At the current state of the art, the most practical approach for turbulence simulation, and the one used in CFD codes and most widely used in applications involving engineering scale systems, is based on Reynolds Averaging of the Navier Stokes equations (RANS models).

Although no single existing RANS turbulence model predicts a sufficiently wide range of flows with accuracy adequate for engineering needs, at this time for most flows the k- ϵ models seem to be the best choice.

The objective of this work was to assess the predictive power and computational efficiency of a CFD code in the analysis of a challenging single-phase light water reactor problem, as well as to identify areas where further improvements are needed. For the simulation of turbulence a number of k- ϵ models were evaluated, including the standard high Reynolds (Re) number model, the quadratic high Re number model, the low Re number model, the RNG model, and a two-layer model.

In this work, the commercial CFD code STAR-CD was used.¹ STAR-CD is a 3-D single-phase and multiphase code based on an unstructured grid. Turbulence is simulated with a number of variants of the two-equation k- ϵ model. For advection a number of schemes are provided, including first-order upwinding, central differencing, combinations of first-order upwinding and central differencing, and MARS (Ref. 1). The latter is a gradient-based total variation diminishing, second-order accurate scheme. In this work, analyses were performed with MARS as well as with first-order upwinding, and a combination of first-order upwinding and central differencing.

2.0 THE BENCHMARK EXPERIMENTS

The available experimental turbulence data for the evaluation of turbulence models for flows in reactor fuel bundles is very limited. For this work, the Pacific Northwest Laboratories' experiments² on "Effects of Sleeve Blockages on Axial Velocity and Intensity of Turbulence in an Unheated 7 x 7 Rod Bundle" were chosen. They provide a severe test for the validation of core fluid dynamics computer codes in a realistic reactor subassembly geometry. These experiments were performed in the mid-1970s with a 7 x 7 rod bundle consisting of 0.996-cm-diam rods with a pitch of 1.369 (Fig. 1). Sleeve blockages were placed on the center nine rods of the bundle to achieve 70 and 90% flow area reductions in the center four subchannels. These blockages were characteristic of fuel clad "swelling" or "ballooning" that may occur during a loss-of-coolant accident in pressurized water reactors. Axial components of the local mean velocity and local intensity of turbulence were measured using a one-velocity component laser Doppler anemometer. The experiments were performed in water at 29.4° C and with Reynolds numbers of 1.4×10^4 , 2.9×10^4 , and 5.8×10^4 . In this work, the experiments with the unblocked bundle, and with 90% blockage were simulated, and code predictions were compared with measurements. The 90% blockage induced very significant cross flows, and is a more severe test than the 70% blockage. An inlet velocity of 1.74 m/s was used, which corresponds to a Reynolds number of 2.9×10^4 . The significant features of the flow were not significantly dependent on the Reynolds number.²

The experimental data indicates that about twelve hydraulic diameters downstream of the first spacer the velocity profile had nearly recovered from the effects of the spacer. The measurement uncertainty for the axial velocity was $\pm 11\%$ for a nominal velocity value of 1.74 m/s. The uncertainty for the intensity of turbulence was $\pm 16\%$ for a nominal value of 0.132.

3.0 WHOLE BUNDLE SIMULATIONS

Two sets of experiments were simulated: (a) bundle without a blockage, and (b) bundle with 90% blockage. In both cases, symmetry was exploited and only one eighth of the bundle (Fig. 1) was modeled. Because the area of interest is between the first and second spacer, and because the spacers have a significant effect on the flow, the section of the bundle from 25 cm upstream of the first spacer to half way between the second and third spacers was simulated (see Fig. 1). Computations were performed with a reference grid of about 164,000 computational cells. The spacer grids are made of a simple "egg crate" type structure. Four "dimples" contact each rod to firmly hold it in place. The spacer grids were simulated as plates having a zero thickness. Reference 2 that documents the PNL experiments provides no geometric information on the "dimples" and they were ignored in the simulations. In these analyses, for the simulation of turbulence the high Re number k-ε model was used. In this model, it is required that the distance to the wall of the center of a cell adjacent to a wall to be between about 30 and 100 y+, where y+ is the non-dimensional distance based on the shear stress at the wall. This requirement sets a limitation on how fine the grid can be in the gap between two rods. Also, it is difficult to satisfy this requirement in areas inside and near the blockage, where the applicability of the high Re k-ε model is limited from other considerations too. Finally, computations were also performed with a finer grid of about 640,000 by refining the grid in the main flow direction and in locations where the requirements of the distance to a wall were not violated. This grid refinement had no significant impact on simulation predictions.

In the comparison between axial velocity predictions and measurements, the velocity is normalized by the average bundle velocity. A k-ε model does not provide information to directly compute the components of turbulence intensity. It computes the turbulent kinetic energy k given by

$$k = \frac{1}{2} \left(\overline{u_f^2} + \overline{v_f^2} + \overline{w_f^2} \right)$$

where u_f , v_f and w_f are the fluctuations of the velocity components in the main and lateral flow directions, respectively. In this section, the assumption was made that the contribution to turbulent kinetic energy of the fluctuations of the lateral components of velocity is negligible. With this assumption, the axial turbulence intensity is

$$\frac{\left(\overline{u_f^2} \right)^{1/2}}{\bar{u}} = \frac{(2k)^{1/2}}{\bar{u}} \quad (1)$$

where \bar{u} is the mean local axial velocity. A correction to this assumption will be discussed later.

Comparisons of code predictions with measurements were made for the normalized-mean axial velocity (local mean velocity/average velocity at the bundle inlet) and axial turbulence intensity at points on a line perpendicular to the bundle wall (see broken line in Fig. 1) and on planes perpendicular to the direction of the main flow at different distances from the lower spacer, or the blockage centerline.

3.1 BUNDLE WITHOUT BLOCKAGE

Figure 2 shows predictions and measurements of mean axial velocity at 0.017 m downstream of the first spacer. This is the closest distance from the spacer at which measurements were made. Figure 3 shows similar data at 0.309 m downstream of the spacer. At this distance (22 hydraulic diameters from the spacer) the velocity profile has recovered from the effects of the spacer. The agreement between predictions and measurements is good. At both locations the maximum discrepancy between predictions and measurements is about 11%, equal to the maximum measurement uncertainty. Figures 4 and 5 show distributions of the axial turbulence intensity at 0.017 m and 0.309 m downstream of the first grid spacer. Away of the bundle wall, the measured turbulence intensity is: about 13 % immediately downstream of the spacer; and about 5% far downstream of the spacer. The turbulence intensity predictions, as computed from Eq. 1, are in good agreement with measurements just downstream of the spacer, but they are greatly off far downstream of the spacer (Fig. 5). This will be discussed more extensively later.

3.2 BLOCKED ROD-BUNDLE

In this experiment, the geometry of the blockage is such that in the location of maximum blockage the flow area is reduced to 10% of the unblocked subchannel flow area (Fig. 1). The length of the blockage is 8.89 cm. Velocity measurements were made at different distances from the blockage center line (line perpendicular to the main flow direction).

Figures 6 and 7 show velocity predictions and measurements at -0.03 m (upstream) and +0.03 m from the blockage center line. In the area inside the blockage “mouth” there is some flow recirculation. Away from the blockage the agreement between predictions and measurements is good, but there are significant discrepancies inside the blockage. Figures 8 and 9 show data at 0.063 m and 0.089 m downstream of the blockage centerline. The agreement between predictions and measurements is good. It can be seen that the flow distribution starts to recover as we move away of the blockage. Figures 10 and 11 show data at 0.185 m and 0.64 m downstream of the blockage center line. At 0.185 m (13 hydraulic diameters) the flow is still in transition. At 0.64 m (~46 hydraulic diameters) the velocity profile has essentially recovered from the effects of the blockage. The agreement between predictions and measurements is reasonably good. Figure 12 shows turbulence intensity data at 0.03 m upstream of the blockage centerline. Away of the blockage (in the lateral direction) there is good agreement between predictions and measurements, but close to the blockage there is a large discrepancy between predictions and measurements.

4.0 ASSESSMENT OF TURBULENCE MODELS

In the CFD models used in this work, the most significant approximations are those made in the k- ϵ model for the simulation of turbulence. There are many k- ϵ models, although the standard high-Re number model is most widely used. The development of these models is based on approximations supported by a number of different types of flows. Benchmark analyses³ have shown that predictions of a turbulence model can be significantly off in flows that are significantly different from those that were used to support model approximations and determine model constants. The main discrepancies between predictions and measurements presented in this work are attributed to the approximations made in the k- ϵ model. This is supported by the LES simulation presented in Ref. [4] of the PNL experiment without a blockage. In the LES simulation, mean velocity predictions are nearly

identical to measurements. Because of differences in the available k-ε models, an assessment of these models was undertaken for flows in PWR rod bundles. Because there is no information for the detailed geometry of the spacers used in the PNL experiments, in this assessment only the section of the bundle away of spacers was used. In addition to the standard high-Re k-ε model,⁵ the other k-ε models considered are: the quadratic high-Re number model,¹ the low-Re number model,⁶ a two-layer model,⁷ and the RNG model.⁸ In the two-layer model, the “standard” k-ε model is applied everywhere except at near-wall flow regions where a low-Reynolds number turbulence model is used, and the grid structure near a wall is fine enough to resolve the boundary layer.

For this assessment a section of the fuel bundle, as shown in Fig. 13, at the center of the bundle and away from spacer grids (where the effect of the spacers on turbulence has died out) was modeled. For the RNG model, the distance from the wall of the center of the computational cells adjacent to a wall was about $12y^+$, as recommended by the developers of the model.⁸ For the low-Re number model and the two-layer model, this distance was about $1y^+$, and the cell size gradually increased in the direction away of the wall. Indicative of the differences in grid refinement is: for the RNG model, on a plane perpendicular to the main flow direction there were 792 cells, while for the two layer model and the low-Re number model on the same plane there were 2640 cells. Periodic boundary conditions were used in the flow direction, and symmetry boundary conditions were used in the other non-wall boundaries. The simulations were performed on eight processors of a Linux cluster, and were run as steady-state problems. The predictions are the result of the solution of the 3-D Navier-Stokes equations and of the k-ε equations, without the use of any correlations beyond those used in a k-ε model.

Comparisons of code predictions with measurements were made for the axial turbulence intensity and the normalized mean axial velocity (mean local axial velocity/average axial velocity) at points on the axis of symmetry of the model (see Fig. 13) and on a plane perpendicular to the direction of the main flow.

LES simulations of the experiment analyzed here show that the fluctuations of the velocity component in the main flow direction contribute about 60% of the total turbulent kinetic energy. In this assessment, the turbulence intensity in the main flow direction was computed from

$$\frac{(\overline{u_f^2})^{1/2}}{\bar{u}} = \frac{(0.6 \times 2k)^{1/2}}{\bar{u}}$$

where: u_f = fluctuation of axial velocity, \bar{u} = mean local axial velocity, and k = turbulent kinetic energy.

Figures 14 and 15 show axial velocity and turbulence intensity predictions and measurements. All k-ε models predict very nearly the same velocity profile. There is an overprediction around the center of the flow channel (area of velocity peaks) and an underprediction in the gap between the rods (area of velocity dips). The maximum discrepancy between predictions and measurements is about 8%, well within the experimental error. All k-ε models overpredict the turbulence intensity, especially in the region around the gap. The predictions of the RNG and standard k-ε model are nearly identical, while those of the two-layer model are significantly higher. The maximum overprediction of the RNG and standard k-ε models is about 23%.

The computational time per processor was 107 min for the high-Re and RNG models (198,000 computational cells), and 337 min for the two-layer model (660,000 computational cells).

5.0 CONCLUSIONS

Advances in CFD codes and parallel computing hold the promise for adequately accurate simulation of reactor flows at reasonable computational effort. This can significantly reduce the need for expensive experiments for design optimization and conservatism in safety margins. At the current state of the art, the most practical approach for turbulence simulation is the use of a RANS model, and especially of the $k-\epsilon$ type. Analyses with a CFD code of flows in a bundle representative of a PWR rod bundle show that away of components that cause significant flow deflections the agreement of mean velocity predictions with measurements is good. Close to such components the discrepancy between velocity predictions and measurements can be large. These discrepancies are attributed to shortcomings of the $k-\epsilon$ turbulence models. Even in rod bundles without flow deflectors, the turbulence predictions of standard $k-\epsilon$ models are in significant discrepancy with measurements. To improve the fidelity of CFD simulations of flows in reactor rod bundles, the development of RANS turbulence models based on such flows is needed.

REFERENCES

1. STAR-CD Version 3.10 – Methodology – User Guide, Computational Dynamics Limited, 1999.
2. J. M. Creer, D. S. Rowe, J. M. Bates, and A. M. Sutey, “Effects of Sleeve Blockages on Axial Velocity and Intensity of Turbulence in an Unheated 7x 7 Rod Bundle,” BNWL-1965, Battelle Pacific Northwest Labs. (Jan. 1976).
3. S. J. Kline, B. J. Cantwell, G. M. Lilley, “Complex Turbulent Flows: Computation and Experiment,” Proc. 1980-1981 AFOSR-HTTM-Stanford Conf. Complex Turbulent Flows, Stanford, California, September 14-18, 1981.
4. C. P. Tzanos, “Large Eddy Simulation of Flow in LWR Fuel Bundles,” Trans. Am. Nucl. Soc., 85, 261 (2001).
5. B. E. Launder and D. B. Spalding, 1974, “The numerical computation of turbulent flow,” *Comp. Meth. in Appl. Mech. & Eng.*, **3**, p. 269.
6. F. S. Lien, W. L. Chen, and M. A. Leschziner, “Low-Reynolds-Number Eddy-Viscosity Modeling Based on Non-Linear Stress-Strain/Vorticity Relations,” Proc. 3rd Symposium on Engineering Turbulence Modeling and Measurements, Crete, Greece, 1996.
7. L. H. Norris and W. C. Reynolds, “Turbulent Channel Flow with a Moving Wavy Boundary”, Report No. FM-10, Department of Mechanical Engineering, Stanford University, USA (1975).
8. V. Yakhot, S. A. Orszag, S. Thangam, T. B. Gatski, and C. G. Speziale, “Development of Turbulence Models for Shear Flows by a Double Expansion Technique”, Phys. Fluids, A4, No. 7, pp. 1510-1520 (1992).

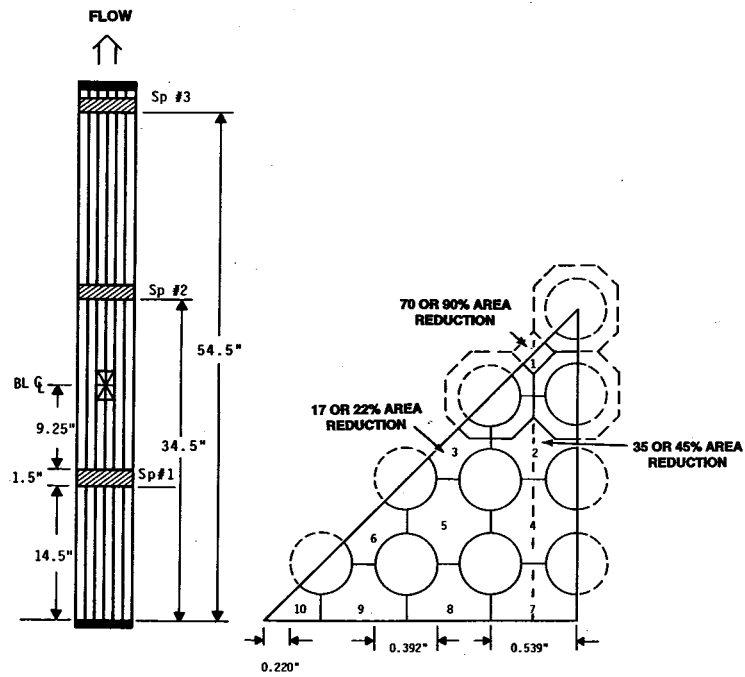


Figure 1. PNL rod bundle

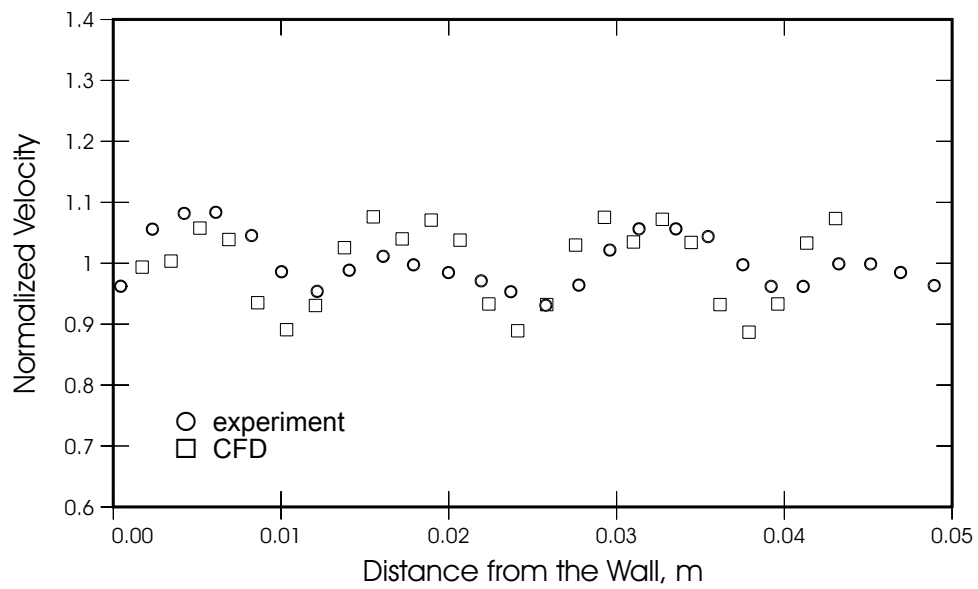


Figure 2. Axial velocity at 0.017 m downstream of spacer

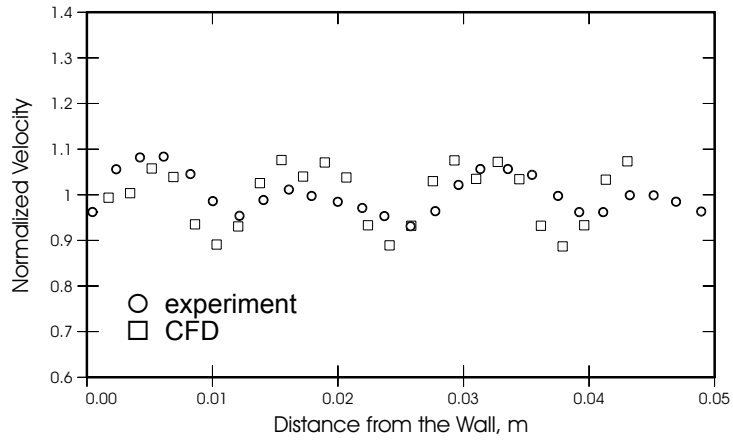


Figure 3. Axial velocity at 0.309 m downstream of spacer

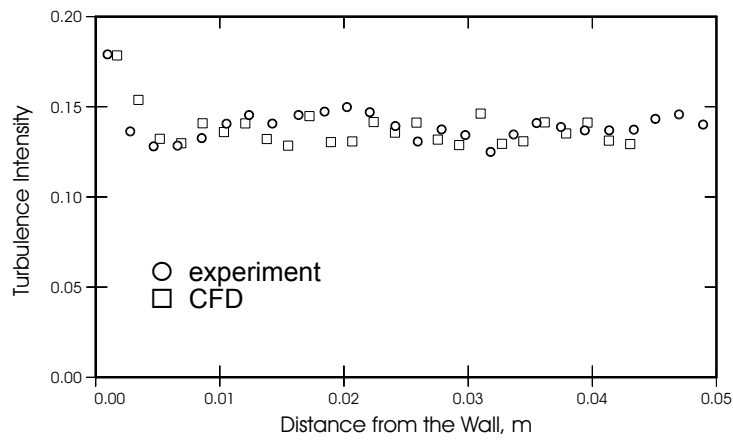


Figure 4. Axial turbulence intensity at 0.017 m downstream of spacer

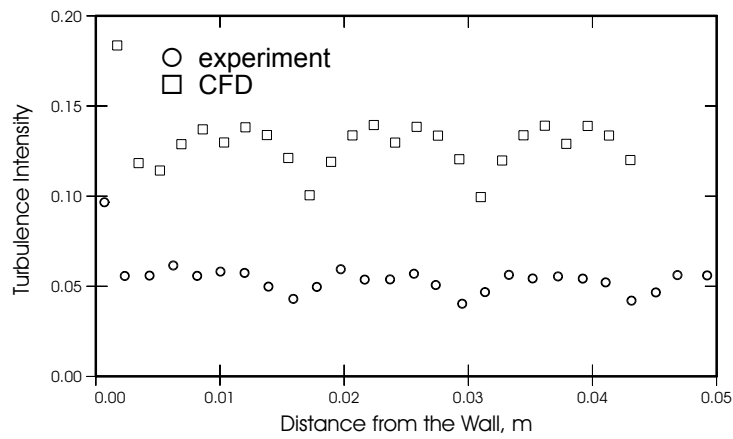


Figure 5. Axial turbulence intensity at 0.309 m downstream of spacer

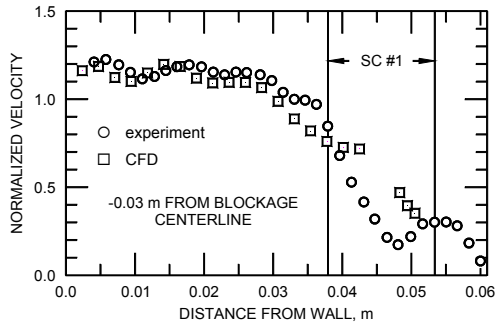


Figure 6. Axial velocity at 0.03 m upstream of blockage centerline.

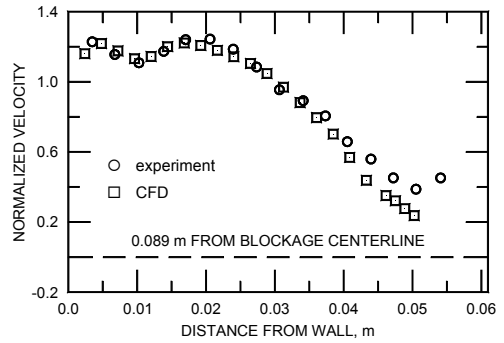


Figure 9. Axial velocity at 0.089 m downstream of blockage centerline.

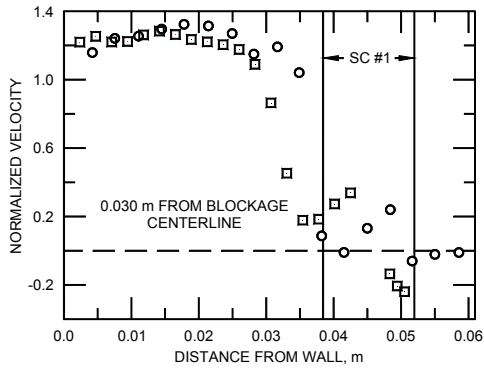


Figure 7. Axial velocity at 0.03 m downstream of blockage centerline.

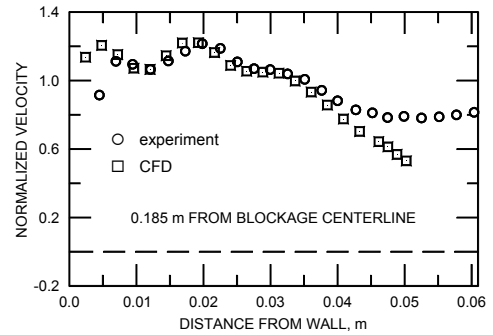


Figure 10. Axial velocity at 0.185 m downstream of blockage centerline.

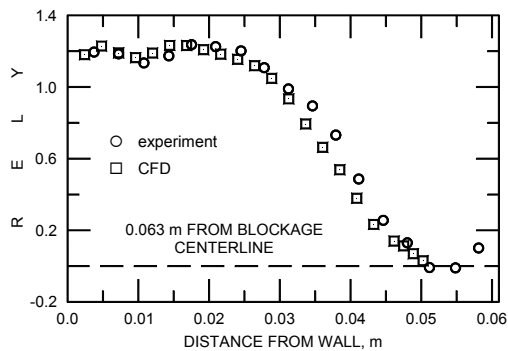


Figure 8. Axial velocity at 0.063 m downstream of blockage centerline.

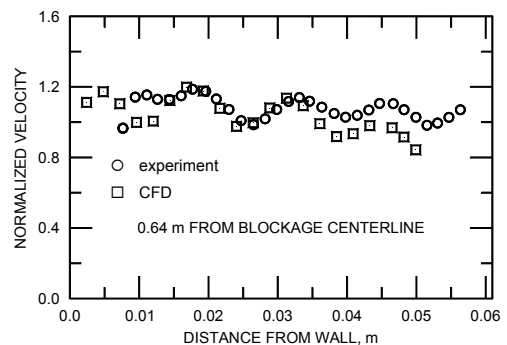


Figure 11. Axial velocity at 0.64 m downstream of blockage centerline.

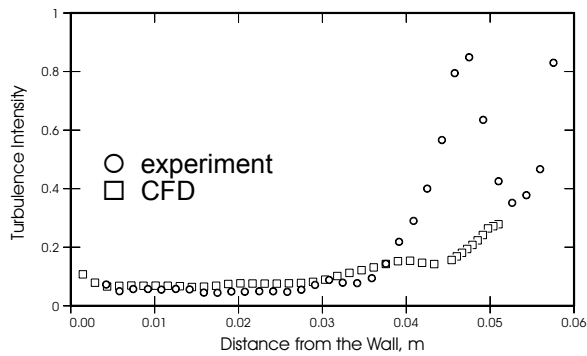


Figure 12. Axial turbulence intensity at 0.03 m upstream of blockage centerline

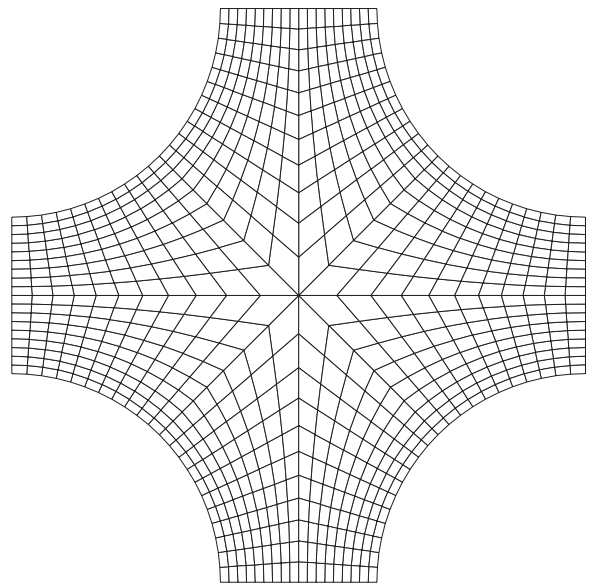


Figure 13. Flow-channel cross section (RNG grid)

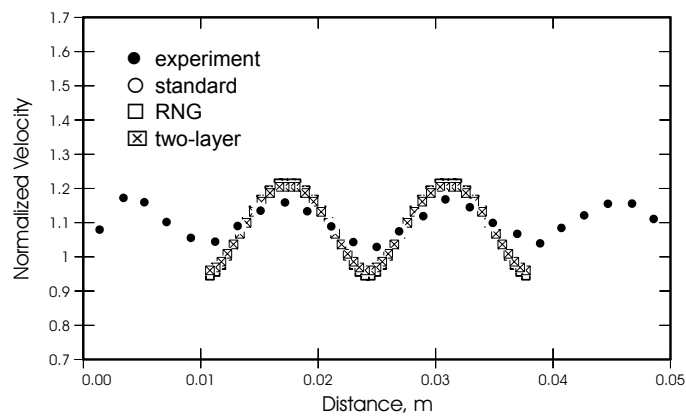


Figure 14. Axial velocity (k- ϵ models vs experiment)

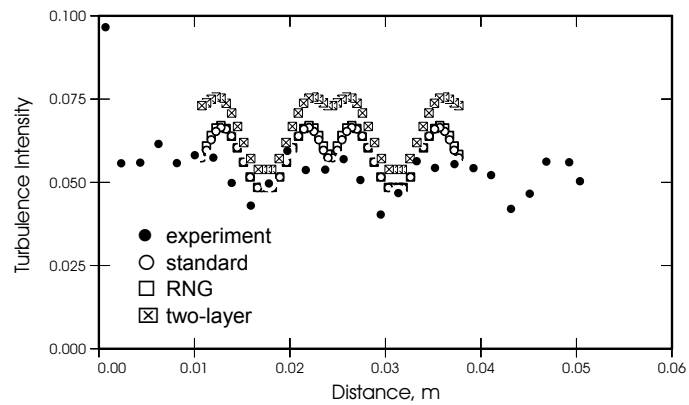


Figure 15. Axial turbulence intensity (k- ϵ models vs experiment)